journal

J. Am. Ceram. Soc., 76 [7] 1681–90 (1993)

Influence of Amorphous Grain Boundary Phases on the Superplastic Behavior of 3-mol%-Yttria-Stabilized Tetragonal Zirconia Polycrystals (3Y-TZP)

Maria Gust,* Grace Goo,* Jeff Wolfenstine,* and Martha L. Mecartney*

Materials Science and Engineering Program, Department of Mechanical and Aerospace Engineering,
University of California, Irvine, California   92717

Amorphous silicate grain boundary phases of varying chemistry and amounts were added to 3Y-TZP in order to determine their influence on the superplastic behavior between 1200° and 1300°C and on the room-temperature mechanical properties. Strain rate enhancement at high temperatures was observed in 3Y-TZP containing a glassy grain boundary phase, even with as little as 0.1 wt% glass. Strain rate enhancement was greatest in 3Y-TZP with 5 wt% glass, but the room-temperature hardness, elastic modulus, and fracture toughness were degraded. The addition of glassy grain boundary phases did not significantly affect the stress exponent of 3Y-TZP, but did lower the activation energy for superplastic flow. Strain rate enhancement was highest in samples containing the grain boundary phase with the highest solubility for Y_2O_3 and ZrO_2, but the strain rate did not scale inversely with the viscosity of the silicate phases. Grain boundary sliding accommodated by diffusional creep controlled by an interface reaction is proposed as the mechanism for superplastic deformation in 3Y-TZP with and without glassy grain boundary phases.

I.   Introduction

SUPERPLASTICITY in ceramics, generally associated with uniform strains over 100%, has generated much interest since Wakai *et al.*[1] first demonstrated superplasticity in 3-mol%-yttria-stabilized tetragonal zirconia polycrystals (3Y-TZP). Structural ceramics such as alumina,[2,3] Si_3N_4,[4] Si_3N_4/SiC,[5] and TZP composites with alumina and mullite[6–11] have all been shown to exhibit superplasticity if processed appropriately. Achieving superplasticity in ceramics allows for net shape forming of components, saving time and money over the traditional practice of sintering and machining. One difficulty with the superplastic deformation of ceramics is that the stresses and temperatures required are often too high to make superplastic forming practical. Thus, it is desirable that superplasticity be obtained at lower stresses and temperatures. One method to promote superplasticity at lower temperatures or stresses is to refine the grain size.[4,12] However, most bulk ceramic materials which exhibit superplasticity already have a fine grain size, typically less than 1 μm, and it is difficult to economically decrease the grain size any further. An alternate technique suggested to enhance the superplastic behavior of ceramics is

through the addition of low melting temperature grain boundary phases.[4,13–16]

Studies have shown that for a given temperature, stress, and grain size, the strain rate increases when amorphous or low melting point grain boundary phases are added to Y-TZP.[17,23] These grain boundary phases soften or become liquid at the superplastic deformation temperatures. Although the addition of an amorphous grain boundary phase can have a significant effect on the deformation behavior of Y-TZP at high temperatures, the exact role that the grain boundary phase plays in the superplasticity of Y-TZP is not well known. There are many questions left to be addressed, including the role of the intergranular phase chemistry and volume fraction with respect to superplasticity and whether the room-temperature mechanical properties are degraded upon the addition of these second phases. Consequently, the current detailed study was undertaken to investigate the effects of amorphous intergranular phase additions on the superplastic and room-temperature mechanical behavior of 3Y-TZP.

For this work, the composition and the amount of the amorphous grain boundary phase added to 3Y-TZP were varied. The glasses chosen for this study were barium silicate and borosilicate glasses. These were specifically selected because at the temperatures of interest (a) they did not enhance static grain growth, (b) there was no crystallization of the glass phases, (c) the components of the glasses had negligible solubility in 3Y-TZP, (d) the different glasses had very different solubilities for Y_2O_3 and ZrO_2, and (e) these glasses completely wet the 3Y-TZP grains at the sintering temperature.[24,25] The difference in solubilities was of particular interest for this investigation. Many of the models proposed to explain the mechanism of superplastic flow (and high-temperature deformation in general) for ceramics containing grain boundary phases predict a linear relationship between the strain rate and the solubility of the ceramic in the liquid phase.[13–16,26]

II.   Experimental Procedure

(1)   Sample Preparation

Samples used in this investigation consisted of coprecipitated 3-mol%-yttria-stabilized zirconia (Toya Soda, Atlanta, GA) fabricated with three different compositions: as-received, with no glass additions, 1 wt% (1.6 vol%) barium silicate (BaS) glass powder (Specialty Glass, Inc., Oldsmar, FL) added, and 1 wt% (2.4 vol%) borosilicate (BS) glass powder (Duran glass, Schott Glaswerke, Mainz, FRG) added. The composition of the glasses is shown in Table I. Samples of 3Y-TZP containing between 0.01 and 5 wt% barium silicate glass were also prepared. The as-received 3Y-TZP powder had a total impurity concentration of about 0.1 wt%, with 0.061 wt% Al_2O_3, 0.015 wt% SiO_2, 0.008 wt% Fe_2O_3, and 0.02 wt% Na_2O as the major impurities.

Powders were mixed in 2-propanol, dried, sieved to less than 80 μm, and cold isostatically pressed under a stress of 400

Table I. Chemical Composition of the Glass Additives

| | Composition (mol%) | | | | | | | |
Glass	SiO_2	Al_2O_3	B_2O_3	Na_2O	K_2O	BaO	SrO	As_2O_3
BaS	45.8	2.1	21.6			29.2	0.7	0.5
BS	83.3	1.5	11.2	3.6	0.4			

MPa. Mixing was tried both by attritor milling with ZrO_2 milling media and by a simple paddle stirrer. For these glass additives with a softening temperature between 800° and 900°C, either method provided a very uniform distribution of glass after sintering as shown by SEM and TEM studies. The pressed powders were then sintered at 1400°C in air for 2 h. Densities were measured using the Archimedes method. All samples had a relative density greater than 98%. The final samples were right circular cylinders with a diameter of approximately 2 mm and a height of about 4 mm.

(2) Mechanical Testing

Two types of mechanical tests were used to characterize the superplastic behavior of 3Y-TZP and 3Y-TZP samples containing glass. Constant stress tests were performed to investigate microstructural evolution as a function of strain. Stress change tests were conducted to determine the value of the stress exponent, n. In both tests, the samples were deformed under uniaxial compression in a dead-load creep apparatus at approximately true stress conditions. To ensure constant true stress, load was added at intervals of 0.02 true strain. The amount of load added was based on the assumption that the volume of the sample remained constant during the test and that the deformation was homogeneous. The constant stress tests were conducted in air at 1300°C under a true stress of 15 MPa. The samples were deformed to 100% true strain. In the stress change tests, the stress was increased in increments of approximately 0.10 true strain, with the sample deformed to approximately 40% total true strain. The stress change tests were conducted in air at temperatures from 1200° to 1300°C under true stresses between 15 and 70 MPa. No reaction was observed between the SiC platens and the 3Y-TZP samples with and without glass.

Room-temperature elastic modulus, hardness, and fracture toughness were determined using a microhardness indentation technique.[27,28] The ends of each sample were ground parallel, and one end was polished to a surface finish of 1 μm using diamond paste. X-ray diffraction was used to verify that the sample surface did not transform to the monoclinic phase as a result of grinding and polishing. Vickers and Knoop indentations were applied with a 10-kg load using a microhardness testing machine (Zwick 3212, Zwick GmbH & Co., Ulm).

Viscosity data on glasses fabricated with the composition of the grain boundary phase were also obtained. (Glass preparation and viscosity data provided by Corning Laboratory Services, Corning, NY.)

(3) Microstructural Characterization

Scanning electron microscopy (SEM) and analytical transmission electron microscopy (TEM) were used to characterize the microstructure of the as-sintered and deformed samples. SEM samples were polished with 1-μm diamond paste and thermally etched at 1300°C in air for 50 min. No grain growth due to thermal etching was observed. The linear intercept method was used to determine the grain size. The average intercept lengths were multiplied by 1.56 to determine the true grain size. For TEM, samples were dimpled, ion milled, and carbon coated. Examinations were done at a voltage of 200 keV on an analytical transmission electron microscope (Philips CM 20, Eindhoven, Netherlands) equipped with energy dispersive spectroscopy (EDS) (9800, EDAX International, Prairie View, IL). Some studies were also performed on a dedicated high-resolution transmission electron microscope (HREM) (Akashi 002, Japan) operating at 200 keV. Standard samples of known

Y_2O_3/ZrO_2 and ZrO_2/SiO_2 concentrations were used to determine the experimental proportionality constants (k factors) for EDS.

The solubilities for Y_2O_3 and ZrO_2 in the glass phase were obtained by EDS analyses at triple points. Samples with 5 wt% glass were used for these analyses because the glass pockets in samples with less glass were too small for quantitative EDS analyses. EDS analyses of glass pockets were performed by averaging at least 10 measurements. The EDS results for the glass pockets were normalized assuming that the relative concentrations of SiO_2, Al_2O_3, B_2O_3, etc., in the as-received glass powders remained the same. (No evidence of diffusion of the glass constituents into the ZrO_2 grains was observed by EDS.) Quenched samples were also fabricated to study the solubility of Y_2O_3 and ZrO_2 in the glass phase at high temperatures. Thin samples (200 μm thick) were heated to 1300°C in air for 40 min, then water quenched.

III. Results

(1) As-Sintered Microstructure

The as-sintered microstructures of 3Y-TZP with no added glass, with 1 wt% BaS glass, and with 1 wt% BS glass showed a highly dense material with an equiaxed grain structure for all three types of samples. The true grain sizes of 3Y-TZP, 3Y-TZP with 1 wt% BaS glass, and 3Y-TZP with 1 wt% BS glass were 0.41 ± 0.07, 0.44 ± 0.05, and 0.42 ± 0.05 μm, respectively. No distinct second phases were observed in the scanning electron micrographs for any of the three materials.

Transmission electron micrographs of as-sintered 3Y-TZP with and without glass additions are shown in Fig. 1. No grain boundary phases are observed in 3Y-TZP with no added glass, whereas small glass pockets (indicated by arrows) located at triple points or at four-grain junctions are observed in 3Y-TZP with 1 wt% BaS and in 3Y-TZP with 1 wt% BS. Grains in 3Y-TZP with no added glass are faceted with sharp triple points. Most of the grains in 3Y-TZP with added glass are also faceted with sharp triple points. However, at multiple grain junctions containing the glass phase, the grain corners are rounded. No distinct second phase could be seen in the glass-doped samples along the grain boundaries at low magnification, so high-resolution studies were conducted. Typical high-resolution lattice images of grain boundaries in 3Y-TZP with and without added glass are shown in Fig. 2. At least 10 boundaries in each material were imaged with HREM. No glass phase is observed along the grain boundaries in 3Y-TZP (Fig. 2(A)). Figures 2(B) and 2(C) show examples of the glass phase for the samples with 1 wt% BaS and 1 wt% BS. All grains are surrounded by a continuous layer of an amorphous phase. The thickness of the grain boundary phase, measured along the different boundaries, varied from 0.4 to 0.8 nm. No significant difference in thickness was noted for the two glass compositions.

(2) Grain Boundary Phase Properties

Solubilities for Y_2O_3 and ZrO_2 in the BaS and BS glass phases in as-sintered and quenched samples are listed in Table II. Both glasses have a higher solubility for ZrO_2 than for Y_2O_3. The BaS glass has a higher solubility for both Y_2O_3 and ZrO_2 than the BS glass. The ZrO_2 concentrations are 2–3 times higher in the BaS glass phase than in the BS glass phase. The Y_2O_3 solubility in the BS glass was much less than that for the BaS glass, in fact was too low to detect using EDS (<1 mol%).
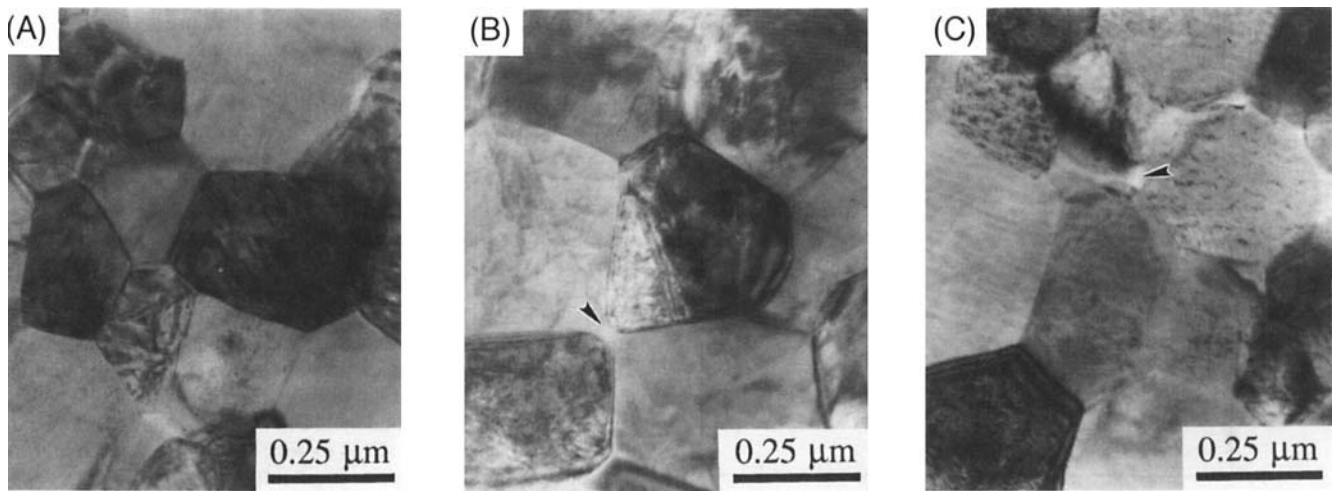
Fig. 1. TEM micrographs of as-sintered 3Y-TZP: (A) without glass, (B) with 1 wt% BaS glass, and (C) with 1 wt% BS glass. Arrows indicate glass pockets at multiple grain junctions.

Quenched samples were fabricated to detect if there were any differences between the grain boundary phase composition at the deformation temperature of 1300°C and the grain boundary phase composition after cooling slowly to room temperature. The solubility for Y_2O_3 and ZrO_2 after quenching from 1300°C

Fig. 2. HREM micrographs of typical grain boundaries in as-sintered 3Y-TZP: (A) without glass, (B) with 1 wt% BaS glass, and (C) with 1 wt% BS glass.

is not significantly different from the solubility in the as-sintered condition for the BS glass, whereas the BaS glass in the quenched sample has a slightly higher solubility for ZrO_2 and a slightly lower solubility for Y_2O_3. Calculating in the dissolved Y_2O_3 and ZrO_2, the volume of the glass phase increased from 1.6 to 2.1 vol% for the BaS samples and from 2.4 to 2.6 vol% for the BS samples, for samples with 1 wt% glass additions.

The viscosity of the BaS and BS glasses with dissolved Y_2O_3 and ZrO_2 is shown in Fig. 3 as a function of temperature. The composition of the glass tested was based on the solubility of 3Y-TZP in the intergranular glass phase averaged for the quenched and slow cooled samples. Although the viscosity of the BaS glass was too low to measure above 1000°C, it can be extrapolated to be several orders of magnitude lower than the viscosity of the BS glass at the temperatures of interest (between 1200° and 1300°C).

(3) High-Temperature Deformation

(A) Compressive Ductility: The superplastic behavior of 3Y-TZP, 3Y-TZP with 1 wt% BaS, and 3Y-TZP with 1 wt% BS samples is shown in Fig. 4. The samples were deformed in compression to 100% true strain at a constant true stress of 15 MPa at 1300°C. A brief normal primary creep stage of about 1% to 2% true strain is observed in all three materials prior to the onset of steady-state behavior. A dramatic enhancement of the strain rate can be seen in the 3Y-TZP samples with added glass. The samples containing glass deformed to 100% true strain in approximately 5 h, whereas the sample with no added glass required approximately 100 h to achieve 100% strain. The sample containing BaS glass had a slightly higher strain rate than the sample containing BS glass. The three materials revealed no evidence of barrelling or edge cracking after 100% true strain.

(B) Deformed Microstructures: Scanning electron micrographs of 3Y-TZP, 3Y-TZP with 1 wt% BaS, and 3Y-TZP with 1 wt% BS samples deformed to 100% true strain at a constant true stress of 15 MPa and temperature of 1300°C (Fig. 4) are shown in Fig. 5. The compressive stress direction is shown by the arrows. The grains remained relatively equiaxed in all three materials and dynamic grain growth was minimal. The true
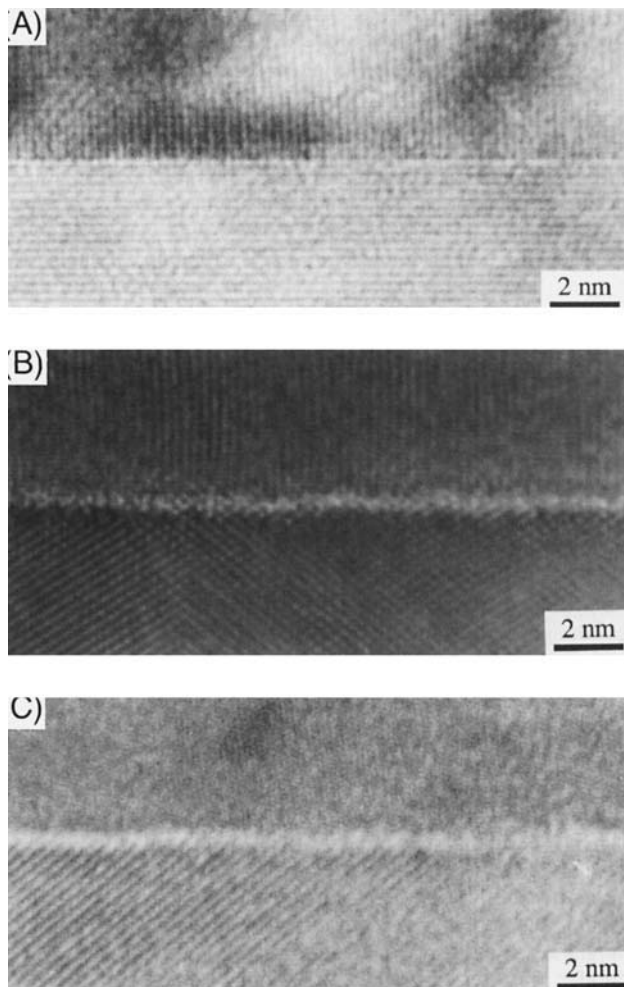
Table II. Y_2O_3 and ZrO_2 Solubility in Glass Phases

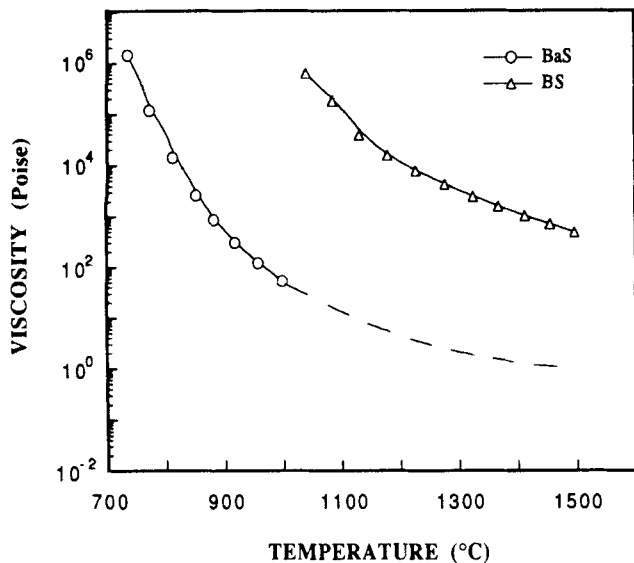|	Y_2O_3 (mol%)	ZrO_2 (mol%)
BaS (undeformed)	4.2 ± 0.7	19.0 ± 2.8
BaS (quenched from 1300°C)	2.3 ± 0.4	23.9 ± 3.2
BS (undeformed)	0.4 ± 0.3	9.7 ± 1.5
BS (quenched from 1300°C)	0.4 ± 0.1	7.9 ± 2.4

Fig. 3. Temperature dependence of the viscosity for the glasses with dissolved ZrO_2 and Y_2O_3. The broken line indicates extrapolated data. (The viscosity of the BaS glass between 1000° and 1500°C was below the detection limit of the equipment.)

grain sizes of the deformed 3Y-TZP, 3Y-TZP with 1 wt% BaS, and 3Y-TZP with 1 wt% BS are 0.54 ± 0.09, 0.51 ± 0.07, and 0.49 ± 0.05 μm, respectively. There was no evidence of cavitation in any of the samples, which density measurements also confirmed.

Transmission electron micrographs of 3Y-TZP, 3Y-TZP with 1 wt% BaS, and 3Y-TZP with 1 wt% BS samples after deformation are shown in Fig. 6. A comparison between the as-sintered microstructures (Fig. 1) and the deformed microstructures (Fig. 6) again reveals that the grains remained equiaxed with minimal dynamic grain growth. The deformed grains appear to be essentially dislocation-free for all three materials. Extensive bend contours are observed in all three materials after superplastic deformation, indicating a high amount of strain in the materials. More bend contours are observed in the sample without glass additions. In addition, some tetragonal grains transformed to monoclinic.

(C) Strain Rate–Stress Relations: The results of the stress change tests for 3Y-TZP, 3Y-TZP with 1 wt% BaS, and
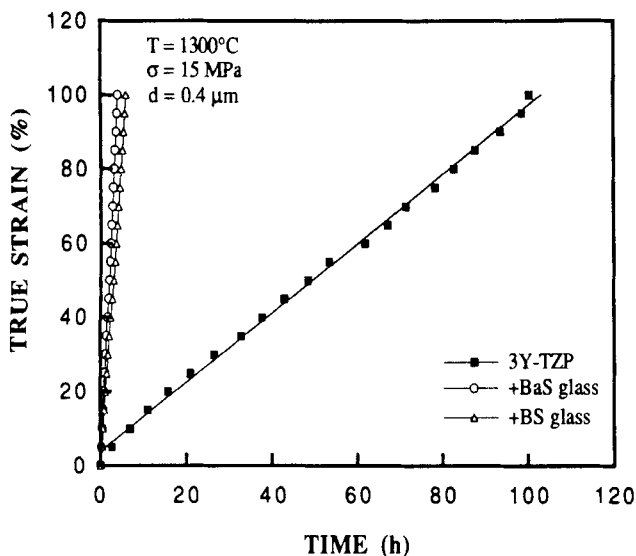

Fig. 4. True strain vs time for 3Y-TZP with and without 1 wt% glass.

3Y-TZP with 1 wt% BS samples at 1300°C are shown in Fig. 7. The data in Fig. 7 are plotted as steady-state strain rate versus applied stress on a logarithmic scale. Both samples with added glass deform much faster than 3Y-TZP with no added glass over the entire range of applied stress. For example, at a given value of stress, 3Y-TZP with 1 wt% glass deforms about an order of magnitude faster than 3Y-TZP with no added glass. The stress exponent, which is the slope of the curves, is about the same for all three materials. The stress exponents for 3Y-TZP with no added glass, with 1 wt% BaS glass, and with 1 wt% BS are 1.8, 1.7, and 1.8, respectively.

Stress change tests were also performed at 1200° and 1250°C on the three materials. At both 1200° and 1250°C, samples containing 1 wt% glass deformed about an order of magnitude faster at a given value of stress than 3Y-TZP with no glass. The stress exponents obtained at 1200°, 1250°, and 1300°C are listed in Table III. The stress exponents for the three materials do not appear to change significantly with temperature. The 3Y-TZP samples containing glass have a slightly lower stress exponent than 3Y-TZP with no added glass at 1200°C and 1250°C.

(D) Activation Energy: The activation energy for superplastic flow for each of the three materials was determined from a plot of logarithm of steady-state strain rate versus inverse temperature at constant stress and grain size. Figure 8 is a plot for data from the stress change tests at a stress level of 35 MPa and grain size of 0.4 μm. The activation energy for superplastic flow, determined from the slope of the straight lines in Fig. 8, is equal to about 640 kJ/mol for 3Y-TZP and 510 kJ/mol for both 3Y-TZP with 1 wt% BaS and 3Y-TZP with 1 wt% BS.

(E) Volume Fraction of Glass Phase: The effect of the amount of glass phase on the superplastic behavior of 3Y-TZP can be seen in Fig. 9. Figure 9 is a plot of logarithm of steady-state strain rate versus logarithm of stress for 3Y-TZP with no added glass and with 0.01, 0.1, 1, and 5 wt% BaS glass at 1300°C and a constant grain size of 0.4 μm. From Fig. 9 it is observed that the strain rate increases at a given value of stress as the amount of glass is increased. The increase in strain rate is not linearly dependent on the amount of glass. For example, at a stress level of 35 MPa, the addition of 5 wt% BaS to 3Y-TZP increases the strain rate by a factor of approximately 25, whereas 1 wt% BaS increases the strain rate by a factor of 7. Note that as little as 0.1 wt% BaS causes the strain rate to increase by a factor of 2. The stress exponent is essentially independent of the amount of glass phase. The stress exponents are 1.8, 2.1, 2.0, 1.7, and 1.9 for 3Y-TZP with no glass and with 0.01, 0.1, 1.0, and 5 wt% BaS, respectively.

(4) Room-Temperature Mechanical Properties

The room-temperature hardness, elastic modulus, and indentation fracture toughness of 3Y-TZP, 3Y-TZP with BaS, and 3Y-TZP with BS containing 1 and 5 wt% glass are listed in Table IV. All the samples have approximately the same grain size of 0.4 μm. From Table IV it is seen that these room-temperature properties are not changed with the addition of 1 wt% glass, but are significantly degraded with the addition of 5 wt% glass of either composition.

IV. Discussion

(1) Microstructure

HREM results of as-sintered 3Y-TZP with and without glass additions (Fig. 2) show the effects of the glass additions on the microstructure. In 3Y-TZP with no added glass, no distinct glass phase is observed either at triple points or along the grain boundaries. Samples with added glass have a continuous intergranular glass phase with a fairly uniform thickness along all high-angle grain boundaries examined by HREM. Although grain boundary phases have commonly been observed in Y-TZP,[19,29–31] studies performed by Nieh *et al.*[32,33] on 2Y-TZP have indicated that Y-TZP materials can be fabricated without
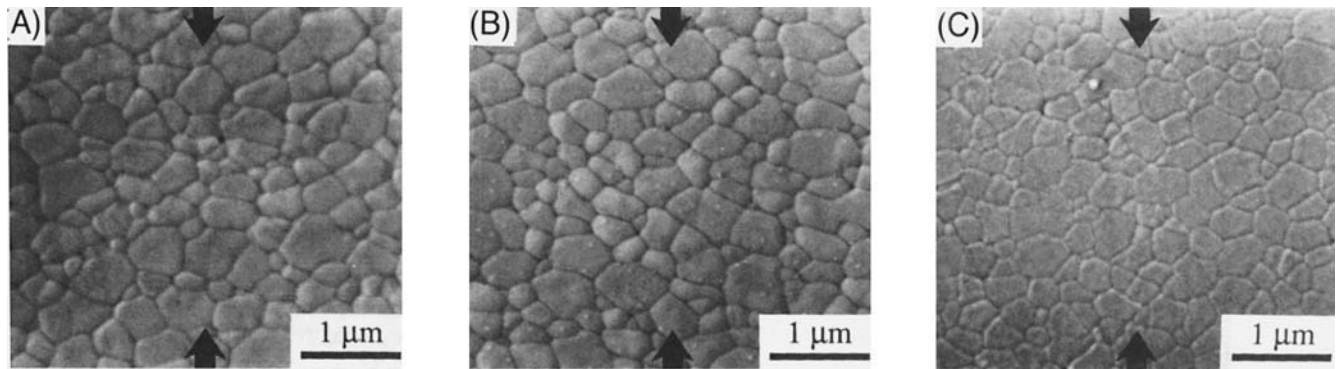
Fig. 5. SEM micrographs of superplastically deformed 3Y-TZP: (A) without glass, (B) containing 1 wt% BaS glass, and (C) containing 1 wt% BS glass. Arrows indicate compressive stress direction.
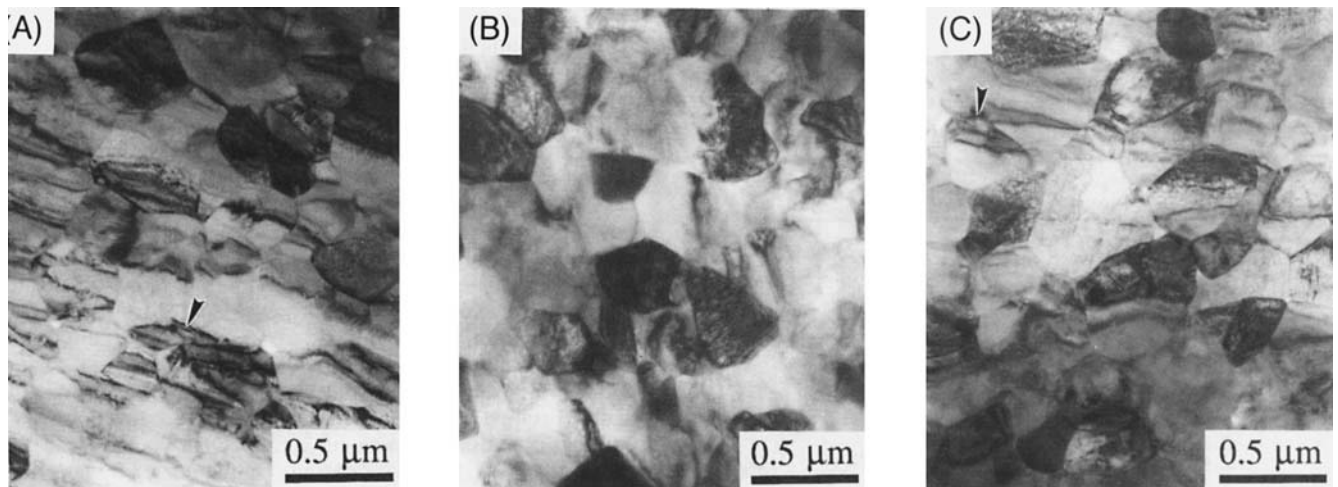

Fig. 6. TEM micrographs of superplastically deformed 3Y-TZP: (A) without glass, (B) with 1 wt% BaS glass, and (C) with 1 wt% BS glass. Arrows indicate areas of monoclinic transformation.

an amorphous grain boundary phase. It has been suggested that the thickness of the amorphous grain boundary phase depends on the chemistry of the intergranular phase as well as on the heat treatment of the ceramic sample.[34-36] For example, the thickness of the amorphous grain boundary phase in Si_3N_4 can

Table III. Stress Exponent (n) of 3Y-TZP with and without Glass Additives

	n at 1200°C	n at 1250°C	n at 1300°C
3Y-TZP	2.0	2.1	1.8
3Y-TZP + 1 wt% BaS	1.7	1.4	1.7
3Y-TZP + 1 wt% BS	1.5	1.6	1.8

range from 0.5 to 2 nm, depending on the composition of the grain boundary phase.[35] In contrast, the BaS and BS glasses used in this investigation formed amorphous films having similar thicknesses in 3Y-TZP, even though the two glasses have very different compositions (Table I).

TEM micrographs of the deformed samples (Fig. 6) reveal bend contours, suggesting a high amount of strain in these samples. Areas of monoclinic transformation are observed, indicating that the stress in the materials was so high in these regions that it nucleated the martensitic transformation from tetragonal to monoclinic. Fewer monoclinic areas are observed in 3Y-TZP with glass than in 3Y-TZP without glass. The intergranular glass phase may help to accommodate residual stresses in the material by allowing grain rearrangement to occur more easily than in 3Y-TZP without glass.

(2) Superplastic Behavior

In general, the superplastic flow of ceramic materials is a diffusion-controlled process where the steady-state strain rate, $\dot{\varepsilon}$, can be expressed as follows:
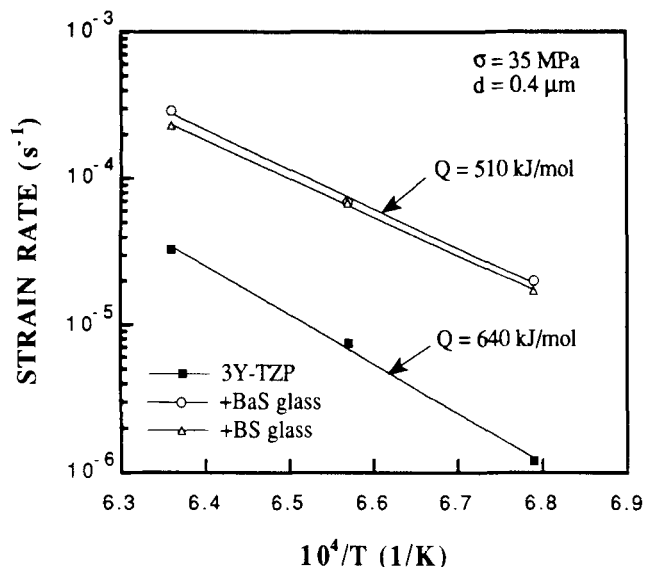

Fig. 7. Steady-state strain rate vs true stress for 3Y-TZP with and without 1 wt% glass.

Fig. 8. Temperature dependence of strain rate for 3Y-TZP with and without 1 wt% glass.
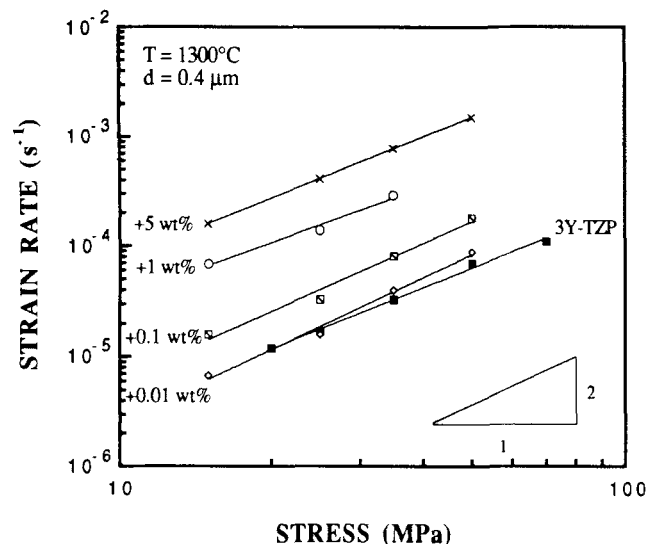

Fig. 9. Steady-state strain rate vs true stress for 3Y-TZP with various amounts of BaS glass.

Table IV. Room-Temperature Mechanical Properties of 3Y-TZP with and without Glass Additives

	H (GPa)	E (GPa)	K_c (MPa·m$^{1/2}$)
3Y-TZP	12.4 ± 0.4	217.5 ± 6.9	4.1 ± 0.1
3Y-TZP + 1 wt% BaS	11.5 ± 0.6	226.3 ± 23.3	3.8 ± 0.2
3Y-TZP + 1 wt% BS	12.6 ± 0.4	219.3 ± 7.0	4.0 ± 0.1
3Y-TZP + 5 wt% BaS	8.2 ± 0.9	153.9 ± 13.6	3.5 ± 0.4
3Y-TZP + 5 wt% BS	8.9 ± 0.3	143.9 ± 3.9	3.1 ± 0.2

$$\dot{\varepsilon} = A\sigma^n d^{-p} \exp\left(-\frac{Q}{RT}\right) \tag{1}$$

where σ is the stress, T is the absolute temperature, d is the grain size, n is the stress exponent, p is the grain size exponent, Q is the apparent activation energy for plastic flow, R is the gas constant, and A is a material constant. The experimental values of n, Q, and p can be compared with theoretical values to determine the rate-controlling deformation mechanism(s).

In the following section, the experimental creep values (n, Q) and microstructural observations for 3Y-TZP containing a grain boundary phase will be compared to the existing models for superplasticity in order to determine the rate-controlling deformation mechanisms in these materials. In addition, the deformation behavior of 3Y-TZP containing two different glasses will be compared in order to gain a better understanding of the importance of grain boundary phase chemistry and volume fraction of glass on the superplastic behavior.

(A) 3Y-TZP: Stress exponent values published for Y-TZP range from 1.0 to 3.5 with activation energies from 360 to 655 kJ/mol.[1,17-23,33,37,38,47] Grain size exponents are not widely documented, but have been reported to be between 1.5 and 2.[20,37,42,47] The large scatter in the n, Q, and p values has been attributed to differences in impurity content, powder processing route, testing technique, and microstructural evolution during deformation.[48] Despite the scatter in these creep parameters, grain boundary sliding has been proposed as one of the most probable mechanisms to explain the superplastic behavior of Y-TZP. The microstructural observations of equiaxed grains in the deformed samples support a grain boundary sliding mechanism.[1,33,37,40-42] Diffusional creep alone would lead to elongated grains.[49]

The many models that exist for grain boundary sliding are summarized in a review paper by Sherby and Wadsworth.[50] Grain boundary sliding must be accommodated by another process in order to keep the grains from separating. It has been proposed that this accommodation can occur by either dislocation motion[51] or diffusional creep.[49] For the case of grain boundary sliding accommodated by dislocation motion, most models predict a stress exponent of 2. In the case of diffusional creep accommodation, the predicted stress exponent is unity when lattice or grain boundary diffusion is rate-controlling. Ashby and Verrall[49] derived an expression for grain boundary sliding and diffusional creep controlled by an interface reaction which contains a stress exponent of 2. Recently, Wakai[45] has suggested that grain boundary sliding accommodated by interface-reaction-controlled diffusional creep may be operable in Y-TZP. In the present study and others,[1,19,33,37,42,45,46] a stress exponent close to 2 has been found for 3Y-TZP with no intergranular glass phase.

For grain boundary sliding accommodated by either dislocation motion or diffusion-controlled diffusional creep, the activation energy for superplastic flow can be correlated with the activation energy for diffusion of the rate-controlling (slowest) species either through the lattice or along the grain boundaries. Diffusion data are not available for 3Y-TZP, so diffusion data for 16-mol%-Y$_2$O$_3$-stabilized ZrO$_2$ have therefore been used for the subsequent discussion. The activation energies for lattice diffusion of the slower-moving cations have been reported to be 391 kJ/mol for Zr^{4+} and 423 kJ/mol for Y^{3+}, while the activation energies for grain boundary diffusion for Zr^{4+} and Y^{3+} have been reported to be 309 and 293 kJ/mol, respectively.[52] The activation energy for superplastic deformation of 3Y-TZP in the present study was 640 kJ/mol, on the high end of the activation energies reported for 3Y-TZP with a similar grain size.[1,20,21,43,44,48] Since the activation energies for superplastic flow are typically much larger than the activation energies for lattice self-diffusion or grain boundary diffusion,[53] this may suggest that during grain boundary sliding, an interface reaction (limiting the rate at which atoms detach and reattach to the grains) is the rate-controlling step.

(B) 3Y-TZP with a Grain Boundary Phase: The exact role that low melting temperature grain boundary phases play in the superplastic behavior of ceramic materials is uncertain. It has been suggested that the liquid phase acts to reduce the friction between the grains, promoting grain boundary sliding, and thus leading to an enhancement in the strain rate.[13] It has also been suggested that the liquid phase acts as a high-diffusivity path compared to grain boundary or lattice diffusion in the diffusional creep process, which also leads to an enhancement in the strain rate.[14-16] In this case, the diffusional creep process for

a polycrystalline material containing a well-dispersed liquid phase is termed solution-precipitation creep.[14-16] Diffusional creep via solution-precipitation alone, however, predicts an elongation of the grains in the direction of the tensile stress.[14-16] This is inconsistent with the equiaxed grains observed after deformation in the present study, so grain boundary sliding must also be occurring.

Strain rate enhancement is observed in 3Y-TZP containing a glassy grain boundary phase (BaS or BS), as shown in Fig. 7. The stress exponent was found to lie between 1.4 and 1.8 for 3Y-TZP containing 1 wt% glass. The similarity of the stress exponents for 3Y-TZP with and without glass suggests that the mechanism of flow may be the same. The observation that the addition of a second phase leads to strain rate enhancement but does not significantly affect the stress exponent agrees with previously published results.[17-23] The grain shapes of the superplastically deformed 3Y-TZP with 1 wt% glass are similar to the grain shapes of the deformed 3Y-TZP without glass (Figs. 5 and 6). The observations of equiaxed grains and no dislocations present after deformation support a grain boundary sliding mechanism for superplastic deformation of 3Y-TZP containing a BaS or BS intergranular phase.

The activation energy for superplastic flow of 3Y-TZP with 1 wt% BaS or BS glass was 510 kJ/mol, lower than 640 kJ/mol found for 3Y-TZP with no added glass. As in the case for 3Y-TZP without glass, we cannot interpret the activation energy for superplastic flow in terms of existing diffusion data. However, a decrease in the activation energy with the addition of a second phase or dopants is consistent with previous reports.[17-23] The lower activation energy for 3Y-TZP with glass than for 3Y-TZP without glass suggests that lattice diffusion is not rate-controlling, since in that case, the activation energy would be the same for both. The lower activation energy in the samples containing glass might indicate the presence of a higher diffusivity path in the liquid grain boundary phase or an easier interface reaction at the liquid/solid interface. It should be noted that the addition of a second phase or dopants does not always lower the activation energy for superplastic flow. An increase in the activation energy has been reported in both 2.5Y-TZP with aluminosilicate glass[18] and in 3Y-TZP containing Al_2O_3 and SiO_2.[19] These increases may be attributed to crystallization of the grain boundary phase (most likely as mullite[24]) or dewetting of the grain boundaries by Al_2O_3 scavenging SiO_2.[54]

The results of Fig. 9 reveal that the strain rate is strongly dependent on the amount of grain boundary phase present for a given grain boundary composition. Hermansson et al.[19] could not observe a direct correlation between the superplastic properties and the volume fraction of glassy grain boundary phase using different compositions for each volume fraction. This emphasizes that superplastic flow is strongly influenced by the grain boundary chemistry and not by the volume fraction of glass alone.

A model which takes into account the influence of the chemistry of the intergranular phase on the high-temperature deformation behavior has been proposed by Raj.[14-16] This model is typically referred to as solution-precipitation creep. Two kinetic processes are involved in this creep deformation mechanism. These two steps are similar to those proposed by Ashby and Verrall[49] for the high-temperature deformation behavior of polycrystalline materials without a liquid phase. First, an interface reaction occurs where atoms are detached from or attached to the grains, and second, atoms are transported along the grain boundaries through the liquid phase. Since these two processes occur sequentially, the slowest is rate-controlling.

If diffusion of atoms through the liquid phase is rate-controlling, the steady-state strain rate is given by a modified Coble creep equation:[55]

$$\dot{\varepsilon} = \frac{A\sigma\Omega C\delta D_l}{kTd^3} \quad (2)$$

where Ω is the atomic volume, C is the solubility of the crystal atoms in the intergranular liquid phase, δ is the thickness of the liquid phase, D_l is the diffusivity of the liquid phase, k is Boltzmann's constant, and A is a constant. Raj[14-16] has modified Eq. (2) for diffusion-controlled solution-precipitation to obtain

$$\dot{\varepsilon} = \frac{2.3\sigma\Omega C\alpha}{\eta d^3} \quad (3)$$

where η is the viscosity of the liquid phase and α is a factor that is proportional to the thickness of the liquid phase.

If the interface reaction is rate-controlling, the equation for the steady-state strain rate derived by Raj[14-16] is given as

$$\dot{\varepsilon} = \frac{k'C\sigma\Omega}{dkT} \quad (4)$$

where k' is the frequency at which solute atoms jump across the interface from the crystal to the liquid.

In examining the equations for solution-precipitation creep, it can be seen that the solubility of the crystal atoms in the liquid phase and the viscosity of the liquid phase play an important role in the deformation behavior. Rather than quantitatively analyzing the strain rates predicted by the model, the relative strain rates observed for 3Y-TZP containing the two different glasses will be examined. At a given value of stress and temperature, all of the terms in Eqs. (3) and (4) are similar for 3Y-TZP containing the two glasses, except the solubility and the viscosity of the glasses. The factor k' may be assumed to be similar for the two liquid/solid interfaces as the activation energies were the same. Therefore, it is possible to express the ratio of the strain rates for the 3Y-TZP materials containing glass in terms of the solubility and the viscosity.

In the case of a diffusion-controlled process (Eq. 3), the ratio of the strain rates is given as follows:

$$\frac{\dot{\varepsilon}_{BaS}}{\dot{\varepsilon}_{BS}} = \frac{C_{BaS}\eta_{BS}}{C_{BS}\eta_{BaS}} \quad (5)$$

Using the solubilities for ZrO_2 (Table II) and the viscosities of the two glasses at 1300°C (Fig. 3), a difference of about 3 orders of magnitude is predicted between the strain rates of 3Y-TZP with 1 wt% BaS glass and 3Y-TZP with 1 wt% BS glass. This predicted difference in strain rates primarily results from the large difference in viscosity between the two glasses. Experimentally, it was observed that the strain rate of 3Y-TZP with 1 wt% BaS glass was only ~1.5 times greater than the strain rate of 3Y-TZP with 1 wt% BS glass (Fig. 7). This large discrepancy between the predicted and observed relative strain rates (1000 vs 1.5) may indicate that this model is not applicable or may arise from several phenomena described in the next paragraph.

The viscosities used in the present study are viscosities of bulk samples of glass and not of thin grain boundary films. Israelachvili et al.[56] and Gee et al.[57] have reported that the viscosity of thin films can be as much as 10^5 greater than the bulk viscosity. Dryden et al.[58] have also reported that the viscosity of a thin liquid phase increases over the bulk viscosity as the reciprocal of the cube of the volume fraction of the liquid phase. However, since the volume fractions of BaS and BS in 3Y-TZP are approximately equal, the thicknesses of the uniform intergranular films are similar, and they are both silicate-based liquids, the relative ratio of the viscosities may remain the same even for the case of thin grain boundary films. Alternately, the thickness of the intergranular film may be different from that measured by HREM. Clarke[36] found that for Si_3N_4, the thickness of the intergranular phase at high temperature was greater than that observed at room temperature, while Badwal et al.[43] have found that the amorphous intergranular phase in Y-TZP can be squeezed out from between the grains during compression. Therefore, the thickness of the intergranular films in 3Y-TZP at high temperature under a compressive stress might be different from the thickness measured at room temperature, although

thickness differences alone would not compensate for the several orders of magnitude difference in viscosity.

In the interface-reaction-controlled process (Eq. (4)), the ratio of the strain rates is given as follows:

$$\frac{\dot{\varepsilon}_{BaS}}{\dot{\varepsilon}_{BS}} = \frac{C_{BaS}}{C_{BS}} \tag{6}$$

Using the solubilities for ZrO_2, the strain rate of 3Y-TZP with 1 wt% BaS glass should be 2–3 times greater than the strain rate of 3Y-TZP with 1 wt% BS glass, in approximate agreement with the observed value of 1.5 times. Therefore, the interface-reaction-controlled case appears to be more consistent in terms of predicting relative strain rates between samples with the same amount of glass but with different glass compositions.

Despite the agreement in predicting the relative strain rates for 3Y-TZP containing two different glasses, there are several discrepancies between the model for solution-precipitation and the experimental data. First, the interface-reaction-controlled process predicts a creep rate that is independent of the amount of grain boundary phase. This is in contrast to the experimental observations which reveal that the strain rate is a function of the volume fraction of glass. For the diffusion-controlled case, the strain rate should be proportional to the thickness of the liquid phase. However, it has been proposed that an equilibrium thickness of amorphous intergranular films exists in ceramics, with the excess glass going into multiple grain junctions.[34] Therefore, the thickness of the intergranular glass phase should be the same in 3Y-TZP containing different amounts of BaS glass. By our calculations, the grains will be coated with a uniform grain boundary layer if 0.1 wt% or more glass is added, considering the initial impurities already present in the 3Y-TZP powders. (In the 3Y-TZP with added glass, only low-angle grain boundaries appeared free of any glassy phase, but the glass appeared to be uniformly distributed along all high-angle grain boundaries.) Therefore, the diffusion-controlled process also cannot explain the increase in the strain rate with an increase in the volume fraction of glass since the thickness of the grain boundary phase should remain the same. Second, both the interface-reaction and diffusion-controlled processes described by Raj predict a stress exponent of unity, whereas the experimental values are closer to 2, although Hwang and Chen[17] have suggested that interface-reaction-controlled solution-precipitation creep should exhibit a stress exponent of 2.

The absence of dislocations after deformation, a stress exponent value of 2, an equiaxed grain structure after deformation, and the direct dependence of the strain rate on the solubility of the glass phase support a grain boundary sliding mechanism accommodated by diffusional creep via interface-controlled solution-precipitation for 3Y-TZP with amorphous grain boundary phases. One flaw with this model for superplastic deformation is that the influence of the volume fraction of glass is not included. If we consider that the accommodation process to prevent grain separation during grain boundary sliding occurs only at multiple grain junctions, then the interfacial area of the grain boundary phase at multiple grain junctions is an important parameter influencing the strain rate. Increasing the volume fraction of glass would increase the strain rate by generating more interfacial area for the interface reaction at multiple grain junctions. The increase in the strain rate should be proportional to the increase in the volume fraction of glass to the 2/3 power from geometrical considerations, since (surface area) is proportional to (volume)$^{2/3}$. The data in Fig. 9 follow this trend. For example, increasing the amount of BaS glass added from 1 to 5 wt% (a 5 times increase in volume) increases the strain rate by 2.3 to 3.4 times for the different stresses, in approximate agreement with the predicted 2.9 (5$^{2/3}$) times increase in strain rate. This relationship assumes that most of the glass exists in multiple grain junctions and would break down when the volume of glass is equivalent or less than that required to coat the grain boundaries with an equilibrium thickness.

(3) Room-Temperature Mechanical Properties

The greatest enhancement in strain rate is observed in 3Y-TZP with 5 wt% BaS glass (Fig. 9). However, the room-temperature hardness, elastic modulus, and fracture toughness are degraded by the addition of such a large amount of glass (Table IV). The degradation in the hardness and elastic modulus is much larger than would be predicted by the rule of mixtures. Yoshizawa and Sakuma[18,22] also observed dramatic strain rate enhancement between 1200° and 1400°C with the addition of 5 wt% of various silicate phases to 2.5Y-TZP, but did not report on the room-temperature hardness, elastic modulus, and fracture toughness. However, they did report a 20% to 30% decrease in the room-temperature bending strength with the addition of glass.[22] Microstructural observations of 3Y-TZP with 5 wt% BaS glass or 5 wt% BS glass have revealed that the ZrO_2 grains are spherical and completely surrounded by the glass phase.[24,25] As a consequence, easy crack propagation through the continuous glassy phase occurs, leading to degraded room-temperature mechanical properties.[25] In contrast, the addition of 1 wt% BaS glass to 3Y-TZP increases the strain rate by an order of magnitude over 3Y-TZP without glass and does not degrade the measured room-temperature mechanical properties.[25] Hwang and Chen[17] have also reported that the addition of less than 1 wt% of low melting temperature CuO to 2Y-TZP enhances the strain rate without significantly affecting the hardness and fracture toughness. Consequently, there appears to be an optimum amount (near 1 wt%) of an amorphous intergranular phase for which the greatest strain rate enhancement is achieved without affecting the room temperature mechanical properties of 3Y-TZP.

V. Conclusions

(1) 3Y-TZP samples can be fabricated with or without a continuous intergranular amorphous phase.

(2) Strain rate enhancement is observed between 1200° and 1300°C in 3Y-TZP containing an intergranular BaS or BS glass phase. The degree of enhancement is dependent on the volume fraction of glass, with strain rate enhancement observed in 3Y-TZP containing as little as 0.1 wt% BaS glass.

(3) The degree of strain rate enhancement depends on the chemistry of the glass phase. For a given stress, 3Y-TZP containing 1 wt% BaS glass has a higher strain rate than 3Y-TZP containing 1 wt% BS glass. The strain rate of the glass-containing samples appears to be proportional to the solubility for Y_2O_3 and ZrO_2, but is not directly related to the viscosity of the glass phases.

(4) The stress exponent is between 1.4 and 2.1 for 3Y-TZP with and without BaS or BS glass. The addition of an intergranular glass phase does not significantly affect the stress exponent of 3Y-TZP.

(5) The activation energy for superplastic flow decreases with the addition of glass. The activation energy for superplastic flow for 3Y-TZP is 640 kJ/mol, whereas the activation energy for superplastic flow for 3Y-TZP containing 1 wt% BaS or 1 wt% BS glass is 510 kJ/mol.

(6) A stress exponent of two along with equiaxed grains after deformation, an absence of dislocations, and an activation energy higher than those for lattice or grain boundary diffusion, suggests that grain boundary sliding controlled by an interface reaction is the mechanism of superplastic flow in 3Y-TZP. Similar results, combined with a lower activation energy for superplastic deformation and a dependence on solubility for 3Y-TZP containing BaS or BS intergranular phases also support a model of grain boundary sliding accommodated by interface-controlled diffusional creep. However, this model does not include a dependence of strain rate on the volume fraction of glass.

(7) If the interface reaction rate is dependent on the interfacial area of the glass pockets at multiple grain junctions, then the strain rate should be proportional to (volume fraction of glass at multiple grain junctions)$^{2/3}$, a relationship in approximate agreement with the experimental results.

(8) The highest strain rate was observed in 3Y-TZP containing 5 wt% BaS glass, but the room-temperature hardness, elastic modulus, and fracture toughness are degraded. The addition of 1 wt% BaS to 3Y-TZP increases the strain rate by an order of magnitude without degrading these room-temperature properties. The addition of a low melting temperature grain boundary phase is a viable means to enhance the superplastic behavior of 3Y-TZP; however, the amount and composition must be carefully chosen in order to obtain the highest strain rate without degrading the room-temperature mechanical properties.

References

[1]F. Wakai, S. Sakaguchi, and Y. Matsuno, "Superplasticity of Yttria-Stabilized Tetragonal ZrO₂ Polycrystals," *Adv. Ceram. Mater.*, **1** [3] 259–63 (1986).

[2]K. R. Venkatachari and R. Raj, "Superplastic Flow in Fine-Grained Alumina," *J. Am. Ceram. Soc.*, **69** [2] 135–38 (1986).

[3]L. A. Xue, X. Wu, and I-W. Chen, "Superplastic Alumina Ceramics with Grain Growth Inhibitors," *J. Am. Ceram. Soc.*, **74** [4] 842–45 (1991).

[4]I-W. Chen and L. A. Xue, "Development of Superplastic Structural Ceramics," *J. Am. Ceram. Soc.*, **73** [9] 2585–609 (1990).

[5]F. Wakai, Y. Kodama, S. Sakaguchi, N. Murayama, K. Izaki, and K. Niihara, "A Superplastic Crystal Composite," *Nature (London)*, **344**, 421–23 (1990).

[6]F. Wakai and H. Kato, "Superplasticity of TZP/Al₂O₃ Composite," *Adv. Ceram. Mater.*, **3** [1] 71–76 (1988).

[7]F. Wakai, Y. Kodama, S. Sakaguchi, N. Marayama, H. Kato, and T. Nagano, "Superplastic Deformation of ZrO₂/Al₂O₃ Duplex Composites"; pp. 259–66 in Superplasticity, MRS Conference Proceedings, International Meeting on Advanced Materials, Vol. 7. Edited by M. Doyama, S. S. Somiya, R. P. H. Chang, M. Kobayashi, and F. Wakai. Materials Research Society, Pittsburgh, PA, 1989.

[8]C. K. Yoon and I-W. Chen, "Superplastic Flow of Two-Phase Ceramics Containing Rigid Inclusions-Zirconia/Mullite Composites," *J. Am. Ceram. Soc.*, **73** [6] 1555–65 (1990).

[9]A. H. Chokshi, T. G. Nieh, and J. Wadsworth, "Role of Concurrent Cavitation in the Fracture of a Superplastic Zirconia–Alumina Composite," *J. Am. Ceram. Soc.*, **74** [4] 869–73 (1991).

[10]R. Martinez, R. Duclos, and J. Crampon, "Structural Evolution of a 20% ZrO₂/Al₂O₃ Ceramic Composite During Superplastic Deformation," *Scr. Metall.*, **24** [10] 1979–84 (1990).

[11]T. G. Nieh, C. M. McNally, and J. Wadsworth, "Superplastic Behavior of a 20% Al₂O₃/YTZ Ceramic Composite," *Scr. Metall.*, **23** [4] 457–60 (1989).

[12]O. D. Sherby and J. Wadsworth, "Superplasticity—Recent Advances and Future Directions," *Prog. Mater. Sci.*, **33**, 169–221 (1989).

[13]G. M. Pharr and M. F. Ashby, "On Creep Enhanced by a Liquid Phase," *Acta Metall.*, **31**, 129–38 (1983).

[14]R. Raj and C. K. Chyung, "Solution-Precipitation in Glass Ceramics," *Acta Metall.*, **29**, 159–66 (1981).

[15]R. Raj, "Creep in Polycrystalline Aggregrates by Matter Transport Through a Liquid Phase," *J. Geophys. Res.*, **87** [B6] 4731–39 (1982).

[16]J.-G. Wang and R. Raj, "Mechanism of Superplastic Flow in a Fine-Grained Ceramic Containing Some Liquid Phase," *J. Am. Ceram. Soc.*, **67** [6] 399–409 (1984).

[17]C.-M. J. Hwang and I-W. Chen, "Effect of a Liquid Phase on Superplasticity of 2-mol%-Y₂O₃-Stabilized Tetragonal Zirconia Polycrystals," *J. Am. Ceram. Soc.*, **73** [6] 1626–32 (1990).

[18]Y.-I. Yoshizawa and T. Sakuma, "Role of Grain-Boundary Glass Phase on the Superplastic Deformation of Tetragonal Zirconia Polycrystal," *J. Am. Ceram. Soc.*, **73** [10] 3069–73 (1990).

[19]T. Hermansson, H. Swan, and G. Dunlop, "The Role of the Intergranular Glassy Phase in the Superplastic Deformation of Y-TZP Zirconia"; pp. 3.329–3.333 in Euro-Ceramics, Vol. 3, *Engineering Ceramics*. Edited by G. de With, R. A. Terpstra, and R. Metselaar. Elsevier Applied Science, London, England, 1989.

[20]M. Nauer and C. Carry, "Flow Behaviors at High Temperatures of Yttria Doped Zirconia Polycrystals"; pp. 3.323–3.328 in Euro-Ceramics, Vol. 3, *Engineering Ceramics*. Edited by G. de With, R. A. Terpstra, and R. Metselaar. Elsevier Applied Science, London, England, 1989.

[21]M. Nauer and C. Carry, "Creep Parameters of Yttria Doped Zirconia Materials and Superplastic Deformation Mechanisms," *Scr. Metall.*, **24** [8] 1459–63 (1990).

[22]Y.-I. Yoshizawa and T. Sakuma, "Effect of Grain Boundary Glassy Phase on Superplastic Deformation in ZrO₂-2.5 mol% Y₂O₃ Alloy"; pp. 272–77 in Proceedings of the 1st Japan International SAMPE Symposium. Nikkan Kogyo Shinbun, Tokyo, Japan, 1989.

[23]Y.-I. Yoshizawa and T. Sakuma, "The Strain-Enhanced Grain Growth in Tetragonal Zirconia Polycrystal During Superplastic Deformation"; pp. 251–56 in *Superplasticity in Advanced Materials*. Edited by S. Hori, M. Tokizane, and N. Furushiro. The Japan Society for Research on Superplasticity, Osaka, Japan, 1991.

[24]Y.-J. Lin, P. Angelini, and M. L. Mecartney, "Microstructural and Chemical Influences of Silicate Grain-Boundary Phases in Yttria-Stabilized Zirconia," *J. Am. Ceram. Soc.*, **73** [9] 2728–35 (1990).

[25]Y.-J. Lin, "Silicate Grain Boundary Phases in Yttria-Zirconia"; Ph.D. Thesis. Department of Chemical Engineering and Materials Science, University of Minnesota, Minneapolis, MN, 1990.

[26]R. L. Stocker and M. F. Ashby, "On the Rheology of the Upper Mantle," *Rev. Geophys. Space Phys.*, **11** [2] 391–426 (1973).

[27]G. R. Anstis, P. Chantikul, B. R. Lawn, and D. B. Marshall, "A Critical Evaluation of Indentation Techniques for Measuring Fracture Toughness: I, Direct Crack Measurements," *J. Am. Ceram. Soc.*, **64** [9] 533–38 (1981).

[28]D. B. Marshall, T. Noma, and A. G. Evans, "A Simple Method for Determining Elastic-Modulus-to-Hardness Ratios using Knoop Indentation Measurements," *J. Am. Ceram. Soc.*, **65** [10] C-175-C-176 (1982).

[29]H. Schubert, N. Claussen, and M. Rühle, "Preparation of Y₂O₃-Stabilized Tetragonal Polycrystals (Y-TZP) from Different Powders"; pp. 766–73 in Advances in Ceramics, Vol. 12, *Science and Technology of Zirconia II*. Edited by N. Claussen, M. Rühle, and A. H. Heuer. American Ceramic Society, Columbus, OH, 1984.

[30]M. Rühle, N. Claussen, and A. H. Heuer, "Microstructural Studies of Y₂O₃-Containing ZrO₂ Polycrystals (Y-TZP)"; pp. 352–70 in Advances in Ceramics, Vol. 12, *Science and Technology of Zirconia II*. Edited by N. Claussen, M. Rühle, and A. H. Heuer. American Ceramic Society, Columbus, OH, 1984.

[31]M. L. Mecartney, "Influence of an Amorphous Second Phase on the Properties of Yttria-Stabilized Tetragonal Zirconia Polycrystals (Y-TZP)," *J. Am. Ceram. Soc.*, **70** [1] 54–58 (1987).

[32]T. G. Nieh, D. L. Yaney, and J. Wadsworth, "Analysis of Grain Boundaries in a Fine-Grained, Superplastic, Yttria-Containing, Tetragonal Zirconia," *Scr. Metall.*, **23** [12] 2007–12 (1989).

[33]T. G. Nieh and J. Wadsworth, "Superplastic Behaviour of a Fine-Grained, Yttria-Stabilized, Tetragonal Zirconia Polycrystal (Y-TZP)," *Acta Metall.*, **38** [6] 1121–33 (1990).

[34]D. R. Clarke, "On the Equilibrium Thickness of Intergranular Glass Phases in Ceramic Materials," *J. Am. Ceram. Soc.*, **70** [1] 15–22 (1987).

[35]H.-J. Kleebe, J. S. Vetrano, J. Bruley, and M. Rühle, "TEM Studies of Grain Boundary Films in Si₃N₄ Ceramics"; pp. 930–31 in Proceedings of the 49th Annual Meeting of the Electron Microscopy Society of America. Edited by G. W. Bailey and E. L. Hall. San Francisco Press, San Francisco, CA, 1991.

[36]D. R. Clarke, "High-Temperature Microstructure of a Hot-Pressed Silicon Nitride," *J. Am. Ceram. Soc.*, **72** [9] 1604–609 (1989).

[37]F. Wakai, N. Murayama, S. Sakaguchi, H. Kato, and K. Kuroda, "Deformation of Superplastic Tetragonal ZrO₂ Polycrystals"; pp. 583–93 in Advances in Ceramics, Vol. 24, *Science and Technology of Zirconia III*. Edited by S. Somiya, N. Yamamoto, and H. Yanagida. American Ceramic Society, Westerville, OH, 1988.

[38]D. Dimos and D. L. Kohlstedt, "Diffusional Creep and Kinetic Demixing in Yttria-Stabilized Zirconia," *J. Am. Ceram. Soc.*, **70** [8] 531–36 (1987).

[39]R. Duclos and J. Crampon, "High-Temperature Deformation of a Fine-Grained Zirconia," *J. Mater. Sci. Lett.*, **6**, 905–908 (1987).

[40]R. Duclos, J. Crampon, and B. Amana, "Structural and Topological Study of Superplasticity in Zirconia Polycrystals," *Acta Metall.*, **37** [3] 877–83 (1989).

[41]T. G. Nieh, C. M. McNally, and J. Wadsworth, "Superplastic Properties of a Fine-Grained Yttria-Stabilized Tetragonal Polycrystal of Zirconia," *Scr. Metall.*, **22** [8] 1297–300 (1988).

[42]Y. Okamoto, J. Ieuji, Y. Yamada, K. Hayashi, and T. Nishikawa, "Creep Deformation of Yttria-Stabilized Tetragonal Zirconia (Y-TZP)"; pp. 565–71 in Advances in Ceramics, Vol. 24, *Science and Technology of Zirconia III*. Edited by S. Somiya, N. Yamamoto, and H. Yanagida. American Ceramic Society, Westerville, OH, 1988.

[43]S. Badwal, F. Ciacchi, M. Swain, and V. Zelizko, "Creep Deformation and the Grain-Boundary Resistivity of Tetragonal Zirconia Polycrystalline Materials," *J. Am. Ceram. Soc.*, **73** [8] 2505–507 (1990).

[44]F. Wakai and T. Nagono, "The Role of Interface-Controlled Diffusion Creep on Superplasticity of Yttria-Stabilized Tetragonal ZrO₂ Polycrystals," *J. Mater. Sci. Lett.*, **7**, 607–609 (1988).

[45]F. Wakai and T. Nagano, "Effects of Solute Ion and Grain Size on Superplasticity of ZrO₂ Polycrystals," *J. Mater. Sci.*, **26**, 241–47 (1991).

[46]T. Hermansson, K. P. D. Lagerlof, and G. L. Dunlop, "Superplastic Deformation of Y-TZP Zirconia"; pp. 631–35 in *Superplasticity and Superplastic Forming*. Edited by C. H. Hamilton and N. E. Paton. The Minerals, Metals, and Materials Society, Warrendale, PA, 1988.

[47]F. Wakai, "A Review of Superplasticity in ZrO₂-Toughened Ceramics," *Br. Ceram. Trans. J.*, **88**, 205–208 (1989).

[48]T. G. Nieh, J. Wadsworth, and F. Wakai, "Recent Advances in Superplastic Ceramics and Ceramic Composites," *Int. Mater. Rev.*, **36** [4] 146–61 (1991).

[49]M. F. Ashby and R. A. Verrall, "Diffusion-Accommodated Flow and Superplasticity," *Acta Metall.*, **21**, 149–63 (1973).

[50]O. D. Sherby and J. Wadsworth, "Observations on Historical and Contemporary Developments in Superplasticity"; pp. 3–14 in Materials Research Society Symposium Proceedings, Vol. 196, *Superplasticity in Metals, Ceramics, and Intermetallics*. Edited by M. J. Mayo, M. Kobayashi, and J. Wadsworth. Materials Research Society, Pittsburgh, PA, 1990.

[51]R. C. Gifkins, "Grain-Boundary Sliding and Its Accommodation During Creep and Superplasticity," *Metall. Trans. A*, **7A**, 1225–32 (1976).

[52]Y. Oishi, K. Ando, and Y. Sakka, "Lattice and Grain-Boundary Diffusion Coefficients of Cations in Stabilized Zirconias"; pp. 208–19 in Advances in Ceramics, Vol. 7, *Additives and Interfaces in Electronic Ceramics*. Edited by M. F. Yan and A. H. Heuer. American Ceramic Society, Columbus, OH, 1983.

[53]T. G. Langdon, "Superplastic Ceramics—An Overview"; pp. 3–18 in *Superplasticity in Aerospace II*. Edited by T. R. McNelley and H. C. Heikkenen. The Minerals, Metals, and Materials Society, Warrendale, PA, 1990.

[54]S. Rajendran, J. Drennan, and S. P. S. Badwal, "Effect of Alumina Additions on the Grain-Boundary and Volume Conductivity of Tetragonal Zirconia Polycrystals," *J. Mater. Sci. Lett.*, **6**, 1431–34 (1987).

[55]R. L. Coble, "A Model for Boundary Diffusion Controlled Creep in Polycrystalline Materials," *J. Appl. Phys.*, **34** [6] 1679–82 (1963).

[56]J. Israelachvili, P. McGuiggan, M. Gee, A. Homola, M. Robbins, and P. Thompson, "Liquid Dynamics in Molecularly Thin Films," *J. Phys.: Condens. Matter*, **2**, SA89–SA98 (1990).

[57]M. L. Gee, P. M. McGuiggan, and J. N. Israelachvili, "Liquid to Solidlike Transitions of Molecularly Thin Films Under Shear," *J. Chem. Phys.*, **93** [3] 1895–906 (1990).

[58]J. R. Dryden, D. Kucerovsky, D. S. Wilkinson, and D. F. Watt, "Creep Deformation Due to a Viscous Grain Boundary Phase," *Acta Metall.*, **37** [7] 2007–15 (1989). □